DINAME 2017 - Proceedings of the XVII International Symposium on Dynamic Problems of Mechanics
A. T. Fleury, D. A. Rade, P. R. G. Kurka (Editors), ABCM, São Sebastião, SP, Brazil, March 5-10, 2017

Effects of geometric nonlinearities of shape memory alloy springs on the aeroelastic behavior of a typical airfoil section

Vagner Candido de Sousa[1], **Carlos De Marqui Junior**[1], **Mohammad Elahinia**[2]

[1] Department of Aeronautical Engineering, Engineering School of Sao Carlos, University of Sao Paulo, Sao Carlos, SP, 13566-590, Brazil, vagner@sc.usp.br, demarqui@sc.usp.br

[2] Dynamic and Smart Systems Lab, Department of Mechanical, Industrial and Manufacturing Engineering, The University of Toledo, Toledo, OH, 43606, USA, mohammad.elahinia@utoledo.edu

Abstract: The effects of the pseudoelastic hysteresis of shape memory alloy (SMA) springs with different geometries on the aeroelastic behavior of a two-degree-of-freedom typical airfoil section are investigated in this work. The ratio of the spring coil diameter to the wire diameter (spring index) is changed, yielding diversified levels of nonlinearity of the mechanical response of the SMA springs and, consequently, changing the aeroelastic behavior of the typical airfoil section. The pure shear assumption is employed to model SMA helical springs at small deflections. A two-state unsteady aerodynamic model for small displacements is employed. The deflections of the SMA springs are determined based on the pitch displacement of the typical airfoil section. Both the coil diameter and the wire diameter of the SMA springs are changed (not simultaneously). Two distinct strategies are considered to keep the same elastic restoring moment when changing the spring index: 1) the stiffness is allowed to change (the number of active coils is not modified in this case); and 2) the stiffness is constant (the number of active coils is modified to achieve the same stiffness). This way, the same aeroelastic behavior is obtained in all cases and any modified aeroelastic behavior can, therefore, only be related to the pseudoelastic hysteresis of the SMA springs. The hysteretic damping can decrease the amplitudes of oscillation of the airfoil at the flutter boundary. Overall, the aeroelastic behavior of the typical airfoil section with SMAs undergoing phase transformation is sensitive to the geometric characteristics of the SMA springs and specific configurations lead to enhanced behavior.

Keywords: shape memory alloy, pseudoelastic hysteresis, aeroelasticity, flutter, helical spring

INTRODUCTION

Aeroelastic phenomena such as flutter and limit cycle oscillations (LCOs) can lead to premature damage and failure of aeronautical structures. The literature on aeroelasticity includes studies on the use of smart materials in vibration control problems. Several research groups have investigated the use of piezoelectric materials in active and passive aeroelastic control cases in the last years (Giurgiutiu, 2000). Shape memory alloys (SMAs) have also been pointed out as promising materials for passive damping augmentation in mechanical and aerospace structures (Gandhi and Chapuis, 2002). The hysteretic response of shape memory alloys exhibiting pseudoelasticity provides energy dissipating and damping capabilities for these materials. Therefore, the effectiveness of the pseudoelastic behavior of shape memory alloys has been investigated for passive structural vibration control (Ibrahim, 2008). The effect of pseudoelasticity of SMA springs on the aeroelastic behavior of a typical airfoil section at the flutter speed and post flutter condition was recently reported (Sousa and De Marqui Jr, 2016).

The modeling of a two-degree-of-freedom (2-DOF) typical aeroelastic section with SMA springs introduced to the pitch DOF has been presented in Sousa and De Marqui Jr (2016). Brinson's model is employed in this study to describe the constitutive behavior of the SMA (Brinson, 1993), and the helical spring model follows reference (Liang and Rogers, 1997). The unsteady aerodynamic loads (lift force and pitch moment) are obtained by Jones' exponential approximation to Wagner's indicial function cast in state-space representation (Jones, 1938; Edwards et al., 1979). The effects of pseudoelastic hysteresis of SMA springs on the aeroelastic behavior of the 2-DOF typical airfoil section are discussed for the flutter boundary and post-flutter condition. In general, the unstable post-flutter condition is replaced by stable LCOs of acceptable amplitudes due to the pseudoelastic hysterisis of SMA springs.

A 2-DOF (namely, plunge and pitch) typical aeroelastic section is considered in this study. A linear elastic spring is modeled in the plunge DOF. Two counter-acting SMA helical springs are modeled in the pitch DOF as the nonlinear mechanism of restoring elastic moment. Classical Brinson's phenomenological model with non-constant material functions for SMAs under uniaxial loading is modified by the pure shear assumption (and von Mises criterion) to model SMA helical springs. A linear unsteady aerodynamic model is used to determine the aerodynamic loads (lift and pitch moment). The proposed aeroelastic model with SMA springs is cast into state-space representation along with two augmented aerodynamic states. The resulting coupled equations are solved over time by a fourth-order Runge-Kutta method.

At each time step, the axial deflections of the SMA springs are determined from the pitch displacement of the typical airfoil section. The shear strain (at the perimeter of the coiled SMA wire) is obtained from the axial deflection of the SMA spring. The corresponding nonlinear shear stress and martensitic volume fraction are solved iteratively and the affected martensite-dependent parameters (such as the elastic modulus) are updated.

Regarding the results, the effects of the pseudoelastic hysteresis of the SMA springs with different geometries (wire and coil diameters) on the aeroelastic behavior of the typical airfoil section are of concern. When the spring coil diameter to the wire diameter ratio (spring index) is changed, diversified nonlinear mechanical responses of the SMA springs are obtained and, consequently, the original linear aeroelastic behavior of the typical airfoil section is also modified to a nonlinear behavior. The aeroelastic behavior of the typical airfoil section with SMAs is sensitive to the geometric characteristics of the SMA springs and it is shown that specific configurations lead to enhanced behavior.

MODEL

Shape memory alloy constitutive model

The critical (normal) stresses for phase transformations in SMAs are given in this paper by (Brinson, 1993)

$$\sigma_s^M = \sigma_s^{\min} + C_M (T - M_s) \tag{1}$$

$$\sigma_f^M = \sigma_f^{\min} + C_M (T - M_s) \tag{2}$$

$$\sigma_s^A = C_A (T - A_s) \tag{3}$$

$$\sigma_f^A = C_A \left(T - A_f\right) \tag{4}$$

where σ_s^M and σ_f^M are the critical values of normal stress for the onset and completion of stress-induced phase transformations (forward phase transformation). Conversely, σ_s^A and σ_f^A are the stress values for the onset and completion of the austenitic phase recovery (reverse phase transformation). Additionally, $\sigma_s^{\min}$ and $\sigma_f^{\min}$ are minimum stresses at which stress-induced phase transformations can begin and complete, respectively. C_M and C_A represent the influence of temperature on the critical stresses of forward and reverse transformations, respectively. M_s is the martensite start temperature, A_s is the austenite start temperature and A_f is the austenite finish temperature (defined in the absence of stress). T is the SMA temperature.

The martensitic fraction during a forward phase transformation is given by

$$\xi^{\mathrm{A}\to\mathrm{M}} = \frac{1-\xi_0}{2} \cos\left[\frac{\pi}{\sigma_s^{\min} - \sigma_f^{\min}} \left(\sigma - \sigma_f^M\right)\right] + \frac{1+\xi_0}{2} \tag{5}$$

where ξ_0 is the initial martensitic fraction and when the applied stress increases from σ_s^M up to σ_f^M.

The martensitic fraction during a reverse phase transformation is given by

$$\xi^{\mathrm{M}\to\mathrm{A}} = \frac{\xi_0}{2} \left\{\cos\left[\frac{\pi}{A_f - A_s} (T - A_s^\sigma)\right] + 1\right\} \tag{6}$$

when the applied stress decreases from σ_s^A to σ_f^A and where $A_s^\sigma = A_s + \sigma/C_A$ is the temperature at which the austenitic phase begins to stabilize with applied stress (Brinson, 1993).

Aeroelastic model with SMA springs

The aeroelastic model is a 2-DOF (plunge and pitch displacements) typical airfoil section (Fig. 1(a)). The SMA springs are included in the pitch DOF (replacing the linear torsion steel spring of Fig. 1(a)) at the ends of a rigid shaft passing through the elastic axis of the typical airfoil section (Fig. 1(b)). The plunge and pitch displacement variables are h (positive downward) and α (positive clockwise), respectively; b is the semichord length, x_α is the dimensionless distance from the elastic axis to the center of gravity, k_h is the plunge stiffness per unit length (in the span direction), k_α is the torsional stiffness per unit length (obtained from the SMA springs S_1 and S_2 in Fig. 1(b)), M_α is the aerodynamic pitch moment per unit length (positive clockwise), L is the lift per unit length (positive upward), U_∞ is the airflow speed, and m is the mass per unit length. The lift acts at the aerodynamic center of the typical airfoil section (at its quarter-chord length for subsonic regime), which in our particular case coincides with the position of the elastic axis. In Fig. 1(b), *e.a.* stands for elastic axis while *a.c.* stands for aerodynamic center.

The dimensionless equations of motion for the typical airfoil section with SMA springs in the pitch DOF are

$$r_\alpha^2 \alpha'' + x_\alpha \bar{h}'' + \zeta_\alpha \alpha' + \vartheta(\alpha, \xi_1, \xi_2) = \bar{M}_\alpha \tag{7}$$

$$x_\alpha \alpha'' + \mu \bar{h}'' + \zeta_h \bar{h}' + \bar{h} = -\bar{L} \tag{8}$$

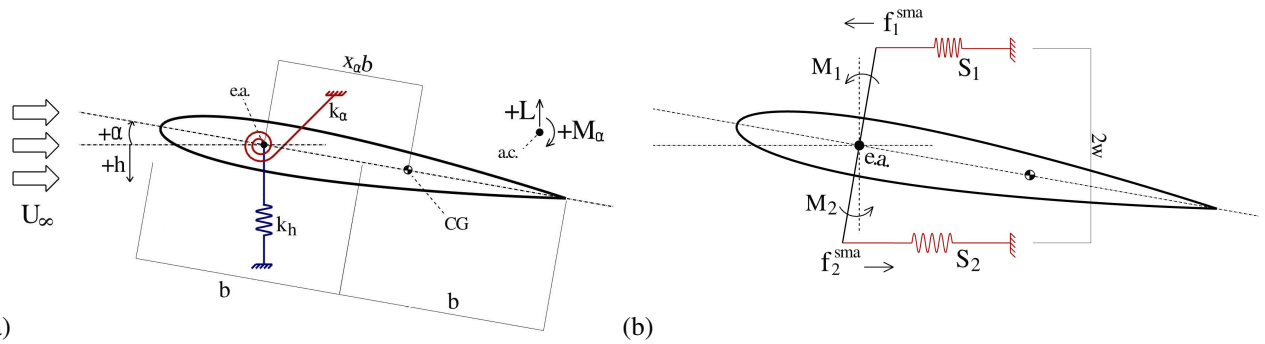

Figure 1 – A typical airfoil section model with ideal (linear elastic) springs (a). A typical airfoil section with helical SMA springs in the pitch DOF (b). The plunge spring is omitted in (b) for clarity purposes.

where $\bar{h} = hb^{-1}$ is the dimensionless plunge displacement, $\mu = (m + m_f)m^{-1}$ is the plunge-to-pitch mass ratio (where m_f is a non-ideal extra mass per unit length in the plunge DOF), $r_\alpha = (I_\alpha m^{-1} b^{-2})^{1/2}$ is the dimensionless radius of gyration, I_α is the moment of inertia per unit length, $\bar{t} = \omega_h t$ is a dimensionless time, where t is the dimensional time, $\omega_h = (k_h m^{-1})^{1/2}$, $\dot{x} = \omega_h x'$ and $\ddot{x} = \omega_h^2 x''$ are the time derivatives, the overdot and the prime denote differentiation with respect to t and $\bar{t}$, respectively, $\zeta_h = d_h(m\omega_h)^{-1}$ is the damping ratio of the plunge DOF and $\zeta_\alpha = d_\alpha(mb^2\omega_h)^{-1}$ is the damping ratio of the pitch DOF, d_h and d_α are the damping coefficients per unit length, $\bar{M}_\alpha = M_\alpha(mb^2\omega_h^2)^{-1}$ is the dimensionless pitch moment and $\bar{L} = L(mb\omega_h^2)^{-1}$ is the dimensionless lift force (Sousa and De Marqui Jr, 2016).

The dimensionless elastic moment due to the SMA springs, from Fig. 1(b), is

$$\vartheta(\alpha, \xi_1, \xi_2) = \frac{w}{mlb^2\omega_h^2}\left[-f_1^{\text{sma}}(\alpha, \xi_1) + f_2^{\text{sma}}(\alpha, \xi_2)\right] \tag{9}$$

where ξ_i is the martensitic fraction of each SMA spring (subscript i assumes 1 for S_1 and 2 for S_2) and w is the distance of each SMA spring from the elastic axis. The forces f_1^{sma} and f_2^{sma} of each SMA spring are

$$f_i^{\text{sma}} = k(\xi_i)\, y_i(\alpha) + Y(\xi_i), \quad i = 1 \text{ or } 2 \tag{10}$$

where $y_i(\alpha)$ denotes the axial deflections of the SMA springs, which are approximated by

$$y_1(\alpha) = y_0 - w\alpha; \quad y_2(\alpha) = y_0 + w\alpha \tag{11}$$

and y_0 is the pre-deflection applied to the springs (yielding preload) in order to bias the stresses towards the phase transformation region.

The stiffness $k(\xi_i)$ of an SMA spring can be represented by

$$k(\xi_i) = \frac{r^4}{4R^3 N} G(\xi_i) \tag{12}$$

where r is the coil spring wire radius, R is the mean coil radius, N is the number of active coils and $G(\xi)$ is the martensite-dependent shear modulus, given by (Liang and Rogers, 1997)

$$G(\xi_i) = G_A + \xi_i(G_M - G_A) \tag{13}$$

where G_M is the fully martensitic shear modulus and G_A is the fully austenitic shear modulus.

The inelastic term related to the hysteretic behavior in Eq. (12) is given by

$$Y(\xi_i) = -\frac{\pi r^3}{2R} G(\xi_i)\, \xi_i \varepsilon_{\text{res}} \tag{14}$$

where ε_{res} is the maximum residual strain of the SMA.

The mechanical constitutive equation of Liang and Rogers (1997) for SMAs under pure torsion is employed here to represent the hysteretic shear stress-strain behavior. The initial state of the aeroelastic problem of this paper is known and thus the axial deflection of each SMA spring is computed at each time step as the numerical solution evolves. The corresponding shear strain of each SMA spring can be estimated by

$$\gamma(y_i, \alpha) = \frac{r}{2\pi R^2 N} y_i(\alpha) \tag{15}$$

which is used in $\tau = G\gamma$ in order to verify if the shear stress is within a transformation range. If so, the actual (nonlinear) shear stress is determined iteratively. Values for the shear stress in the transformation range (denoted by τ_{test}) are used in

Eq. (5) or (6) by considering the von Mises criterion for pure shear, $\sigma = \sqrt{3}\tau_{\text{test}}$ (Liang and Rogers, 1997), yielding to values for ξ_i between 0 and 1, denoted by ξ_{test}. Each pair $(\xi_{\text{test}},\ \tau_{\text{test}})$ is verified in the following equation

$$\tau_{\text{test}} - G(\xi_i)\left[\gamma(y_i,\alpha) - \xi_{\text{test}}\varepsilon_{\text{res}}\right] = 0 \tag{16}$$

which also uses the shear strain obtained by Eq. (15). The state-space representation of the model is omitted here for brevity and can be found in Sousa and De Marqui Jr (2016).

RESULTS

Effects of geometric properties of the SMA springs on the aeroelastic behavior of the typical section (at the linear flutter speed of the original configuration with steel spring in pitch) are investigated in this paper. The considered SMA constitutive properties are displayed in Tab. 1 and are based on Aguiar et al. (2013). The diameter of the SMA wire is 0.95 mm, the mean coil diameter of the spring is 8 mm and the number of active coils is 16.5. The SMA temperature is assumed equal to A_f and the corresponding critical stresses are τ_s^M = 95 MPa, τ_f^M = 135 MPa, τ_s^A = 52 MPa and τ_f^A = 0 MPa. From Eq. (14), the fully austenitic stiffness of each SMA spring is 175 N·m^{-1}. Moreover, the SMA springs are 36.7 mm long and can be compressed up to 20 mm. The distance of each SMA spring from the elastic axis is w = 85 mm. A fourth-order Runge-Kutta method with step size on the order of 10^{-6} s is used.

Table 1 – SMA constitutive properties.

Property	Value	Unit
M_f	302	K
M_s	315	K
A_s	316	K
A_f	331	K
C_M	4	MPa·K^{-1}
C_A	6	MPa·K^{-1}
$\sigma_s^{\min}$	100	MPa
$\sigma_f^{\min}$	170	MPa
ε_{res}	6.7	%
G_M	11.5	GPa
G_A	14.5	GPa
μ_P	0.3	–

The dimensionless aeroelastic parameters are given in Tab. 2 and are based on the experimental parameters of Sousa et al. (2011). An airfoil of 0.125 m semichord length and 0.50 m span length is assumed. An initial plunge displacement of 10 mm (or dimensionless plunge displacement $\bar{h} = 0.08$) is considered in all cases.

Table 2 – Aeroelastic parameters used in the simulations.

Property	Value	Unit
l	0.5	m
b	0.125	m
c	-0.5	–
x_α	0.256	–
m	1.542	kg·m^{-1}
m_f	2.548	kg·m^{-1}
I_α	0.0072	kg·m
k_α	5.08	N·rad^{-1}
k_h	4200	N·m^{-2}
ζ_α	0.088	–
ζ_h	0.0035	–

Aeroelastic behavior of the typical airfoil section with SMA springs

In a previous work, Sousa and De Marqui Jr (2016) report on the effects of preloaded SMA springs on the aeroelastic behavior of a typical airfoil section oscillating at its linear flutter speed. The steady-state plunge and pitch peak amplitudes at the linear flutter speed (11.6 m·s^{-1}) without any preload applied to the SMA springs ($f_0 = 0$ N) are $\bar{h} \approx 0.08$ and $\alpha \approx 0.13$, respectively. This is the linear aeroelastic behavior since no phase transformation is achieved. For the considered configuration, the amplitudes of oscillation decrease for preload values increasing from 2 N to 4.5 N. Such behavior is briefly reviewed in Fig. 2. The predicted attenuation is due to the pseudoelastic hysteresis of the SMAs. Further effects of preload on the plunge and pitch amplitudes are negligible for preload values greater than 3.5 N so that the case of an intermediate preload value (3 N) is discussed in details in the referred paper. The steady-state plunge and pitch

displacements at the same airflow speed and 3 N of preload are $\bar{h} \approx 0.04$ and $\alpha \approx 0.07$.

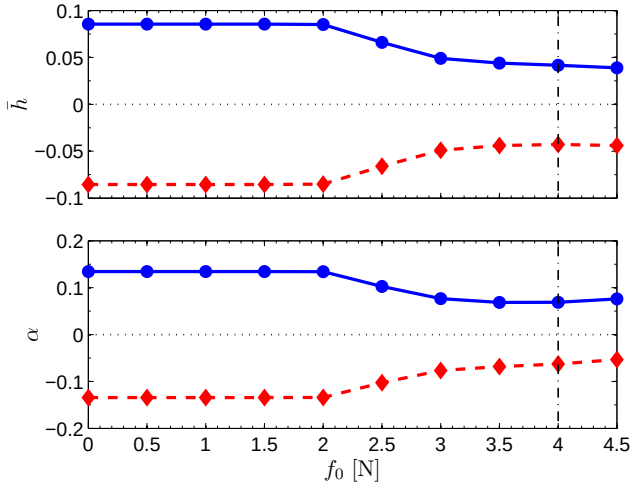

Figure 2 – Steady-state peak amplitudes of the plunge and pitch DOFs at the linear flutter speed for increasing preload values.

Effects of the SMA spring geometry on the aeroelastic behavior of the typical section

An analysis for the identification of physically achievable spring geometries is conducted first. A typical range of helical spring indices C between 4 and 12 is considered. Both the wire diameter (d) and the spring mean coil diameter (D) are modified (not simultaneously) in such a way the index C is in the range of 4 up to 12 considering small increments. Since $C = D/d$, by assuming d constant and equal to its nominal value (0.95 mm), the corresponding coil diameters (D_{var}) range from 3.8 to 11.4 mm. Similarly, for constant D (and equal to its nominal value, 8.0 mm), the range of wire diameters (d_{var}) is between 0.67 and 2.0 mm.

From Eq. (12), two ranges of (austenitic) SMA spring stiffness are obtained for D_{var} and d_{var} as $k_D = [60,\ 1600]$ N·m^{-1} and $k_d = [40,\ 3400]$ N·m^{-1}, respectively and for 16.5 active coils. Please note that k_D and k_d are the spring constants that are combined according to the scheme presented in Fig. 1 to give the pitch stiffness of the typical section. To maintain the same elastic restoring moment in pitch, and therefore the same aeroelastic behavior (assuming all the other parameters constant), the distance w in Fig. 1 has to be adjusted accordingly. However, due to design constraints and also to impractical geometries in an eventual experimental setup, the ranges of stiffness k and distances w have to be limited to a certain range of values.

Fig. 3 displays the spring stiffness (k) and required distance w with the variation of D (Fig. 3(a)) and with the variation of d (Fig. 3(b)). Fig. 3(a) shows that the spring stiffness decreases with increasing spring mean coil diameter (D) and, therefore, w increases with increasing D in order to keep a constant pitch stiffness. On the other hand, the spring stiffness increases with increasing wire diameter (d) and, therefore, w decreases with increasing d in order to keep the resulting pitch stiffness constant.

Another strategy to obtain the same restoring moment in the pitch DOF rather than modifying the distance w is by changing the number of active coils (N) simultaneously to the variation of the spring mean coil diameter or simultaneously to the variation of the wire diameter to keep the nominal SMA spring stiffness. This way, the resulting stiffness, and hence w, are the same despite changes in wire or coil diameters. The number of active coils is calculated by solving Eq. (12) for

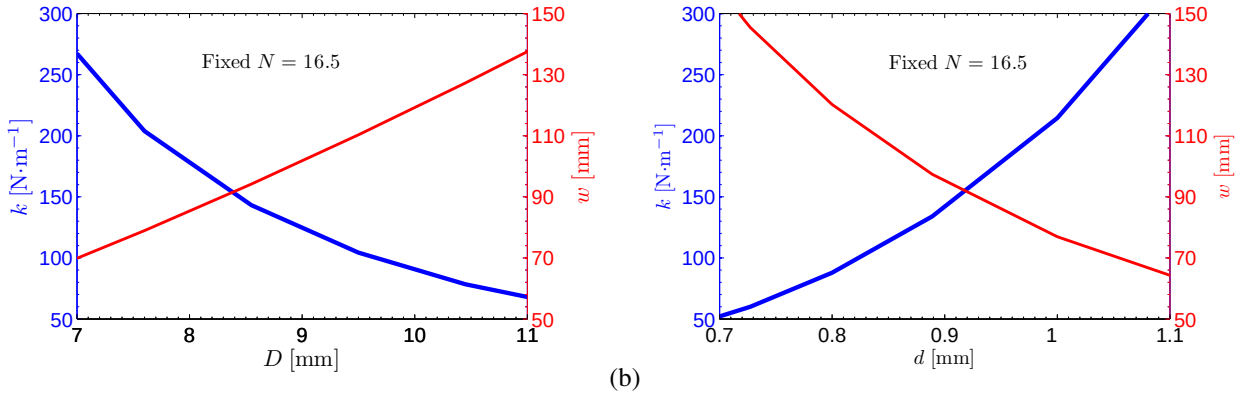

(a) (b)

Figure 3 – SMA spring stiffness (k) and the corresponding distance w between the elastic axis and the SMA springs for increasing coil diameter (a) and wire diameter (b).

N and by using $k = 175$ N·m^{-1} along with D_{var} and d_{var}. Once again neglecting impractical values, Fig. 4 displays the number of coils for varying diameters. The number of active coils decreases with increasing spring mean coil diameter (D) while the number of active coils increases with increasing D, in both cases resulting in a constant spring stiffness and, consequently, the same pitch restoring moment for the typical section.

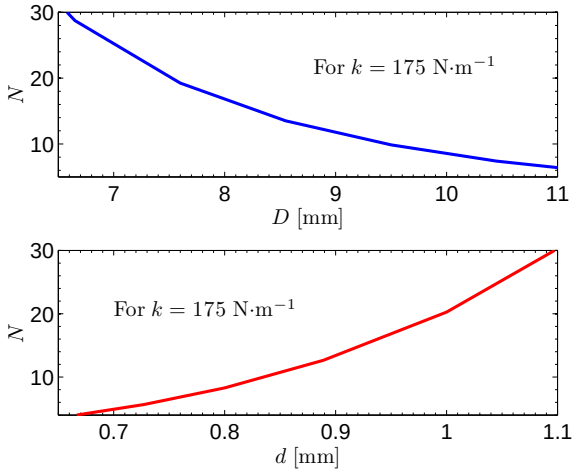

Figure 4 – Number of active coils (N) for varying coil (D) and wire (d) diameters.

Based on Figs. 3 and 4, the analysis of the effects of geometric nonlinearities of SMA springs on the aeroelastic behavior of the typical section is performed for a reduced number of cases, either by assuming D_{var} between 7 mm and 11 mm, or by assuming d_{var} between 0.7 mm and 1.1 mm. In all cases considered in this chapter preloaded SMA springs are considered, so that phase transformations are induced by small pitch displacements. The critical preload (at the imminence of phase transformation) is estimated by solving $\tau = 2FR/(\pi r^3)$ (Liang and Rogers, 1997) for the force in terms of the critical stress (*i.e.,* $F = f_0^{\text{crit}}$ and $\tau = \tau_s^M$).

Fig. 5 displays the steady-state peak amplitudes of the plunge and pitch DOFs at the linear flutter speed of the reference case, both normalized by the aeroelastic response of the reference case (that same of the previous chapters, denoted here as $\bar{h}_{\text{ref}}$ and α_{ref}). The number of coils of the SMA springs in pitch is fixed ($N = 16.5$) and both the resulting stiffness k (due to the variation of D or d, as displayed in Fig. 3) and distance w are changed (corresponding to the cases of Fig. 3) to keep the pitch restoring elastic moment constant. Fig. 5 shows that the pitch and plunge amplitudes increase with increasing D. However, the amplitudes of the preloaded case are always smaller than the amplitudes of the reference case. Moreover, the combination of D = 7 mm and the respective w (from Fig. 3(a)) leads to the smallest pitch and plunge amplitudes. A similar behavior is observed for the variation of d and w in Fig. 5. However, small wire diameter (d) leads to smaller pitch amplitudes than small values of D.

Fig. 6 displays the pitch and plunge peak amplitudes for the case previously discussed in Fig. 4 (spring stiffness kept constant and modifying the number of active coils (and D or d) to keep the pitch stiffness constant. The pitch and plunge amplitudes are always smaller than the amplitudes of the reference case. The amplitudes decrease with increasing D (Fig. 6), and consequently decreasing N (Fig. 4) while the amplitudes increase with increasing d (Fig 6(b)) and decreasing N (Fig. 4).

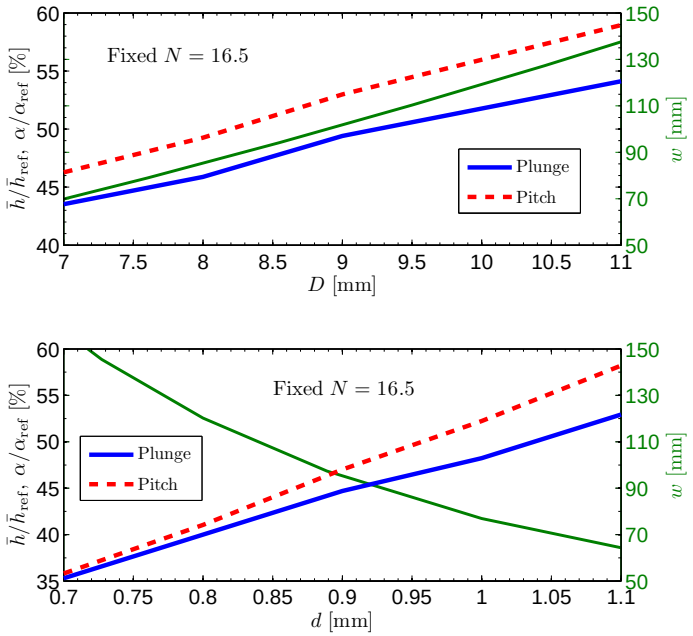

Figure 5 – Steady-state aeroelastic behavior for different SMA spring diameters (with variable stiffness and constant number of coils).

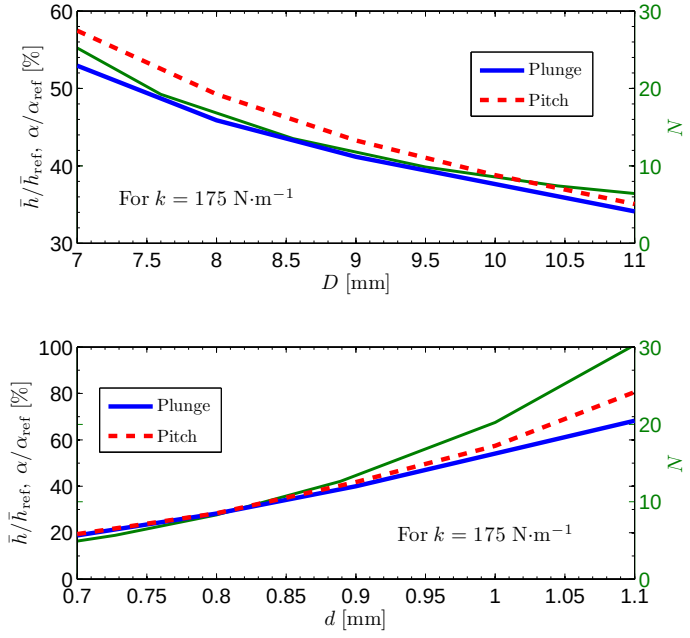

(b)

Figure 6 – Steady-state aeroelastic behavior for different SMA spring diameters (with constant stiffness and variable number of coils).

By comparing the predicted amplitudes of the cases of Figs. 5 and 6, one may note the smallest pitch and plunge amplitudes are obtained in Fig. 6 (for varying wire diameter and the number of coils) for $d = 0.7$ mm and $N = 5$. Decreasing the wire diameter is the most favorable condition to achieve phase transformation and improve the pseudoelastic damping for the case of this discussion. Fig. 7 displays the time response of the plunge and pitch DOFs for three different cases at the linear flutter speed: 1) for the reference case (without preload, which exhibits larger amplitudes), 2) for the nominal geometry with applied preload (which corresponds to the reference case with added preload, and exhibits intermediate amplitudes), and 3) for the case which yields the smallest aeroelastic amplitudes. Clearly, the effect of pseudoelastic hysteresis of the SMA springs on the aeroelastic behavior of the typical section can be enhanced by adjusting the spring geometric properties.

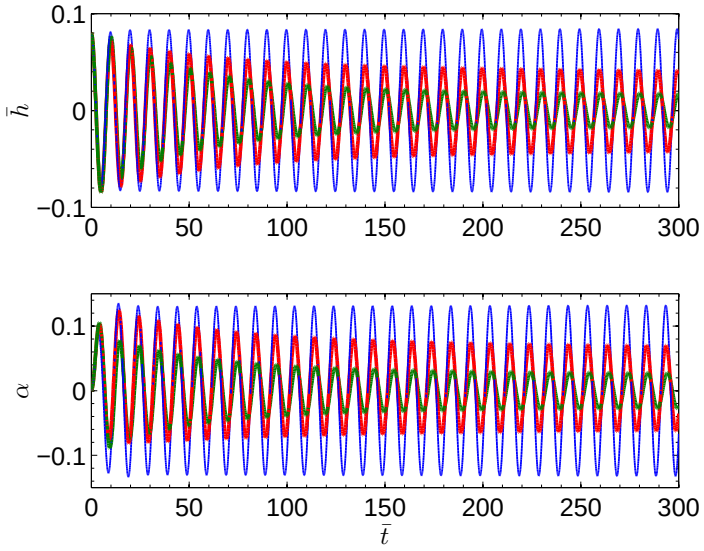

Figure 7 – Time response of the plunge ($\bar{h}$) and pitch (α) DOFs. The largest oscillation (blue line) is the linear case for reference (without preload applied to the SMA springs). The oscillation with intermediate amplitudes (red line) is the case for the nominal spring geometry along with preloaded SMA springs. The smallest amplitudes (green line) is the case for the spring geometry given by d = 0.7 mm and N = 5 along with applied preload.

CONCLUSIONS

The effects of the pseudoelastic hysteresis of shape memory alloy (SMA) springs with different geometries (wire and coil diameters) on the aeroelastic behavior of a two-degree-of-freedom typical airfoil section are investigated. Classical SMA models are modified by the pure shear assumption to represent the SMA helical spring behavior. It is shown that the hysteretic damping can decrease the amplitudes of oscillation of the airfoil at the flutter boundary.

Overall, the aeroelastic behavior of the typical airfoil section with SMAs undergoing phase transformation is sensitive to the geometric nonlinearities of the SMA springs. By considering SMA springs with the same constitutive parameters (made of the same material), springs of lower indices are stiffer and exhibit smaller axial deflections for the same loading. Therefore, although the spring is nonlinear, its behavior is comparable to the behavior of a linear spring. Conversely, higher spring index values are a softening factor which yields larger axial deflections and hence geometric nonlinearity related to more pronounced hysteresis loops. The aeroelastic behavior of the typical airfoil section is discussed for different scenarios. By assuming a set of aeroelastic parameters of a typical airfoil section, the model predicts that the plunge and pitch amplitudes (at the linear flutter speed) decrease about 80%. It is worth noting that the reported improvement is only due to geometric nonlinearity of the SMA springs, which can be combined with a proper choice of SMA constitutive properties (Sousa et al., 2016) along with fabrication routes and heat treatment procedures (Elahinia et al., 2012) to further enhance the aeroelastic behavior of the typical section with SMA springs.

ACKNOWLEDGMENTS

Part of this work was conducted during a scholarship supported by the International Cooperation Program CAPES-PDSE at The University of Toledo. Financed by CAPES – Brazilian Federal Agency for Support and Evaluation of Graduate Education within the Ministry of Education of Brazil (grant number 99999.002891/2015-08).

The financial supports by CAPES [grant number DS-00011/07-0] and the São Paulo Research Foundation (FAPESP) [grant number 2015/26045-6] are also greatly appreciated.

REFERENCES

Aguiar, R.A.A., Savi, M.A. and Pacheco, P.M.C.L., 2013, "Experimental investigation of vibration reduction using shape memory alloys", Journal of Intelligent Material Systems and Structures. Vol.24, No.2, pp. 247-261.

Brinson, L.C., 1993, "One-dimensional constitutive behavior of shape memory alloys: thermomechanical derivation with non-constant material functions and redefined martensite internal variable", Journal of Intelligent Material Systems and Structures. Vol.4, No.2, pp. 229-242.

Edwards, J.W., Ashley, H. and Breakwell, J.V., 1979, "Unsteady aerodynamic modeling for arbitrary motions", AIAA Journal. Vol.17, No.4, pp. 365-374.

Elahinia, M.H., Hashemi, M., Tabesh, M. and Bhaduri, S.B., 2012, "Manufacturing and processing of NiTi implants: A review", Progress in Material Sciences. Vol.57, No.5, pp. 911-946.

Gandhi, F. and Chapuis, G., 2002, "Passive damping augmentation of a vibrating beam using pseudoelastic shape memory alloy wires", Journal of Sound and Vibration. Vol.250, No.3, pp. 519-539.

Giurgiutiu, V., 2000, "Review of smart-materials actuation solutions for aeroelastic and vibration control", Journal of Intelligent Material Systems and Structures. Vol.11, No.7, pp. 525-544.

Ibrahim, R.A., 2008, "Recent advances in nonlinear passive vibration isolators", Journal of Sound and Vibration. Vol.314, No.3-5, pp. 371-452.

Jones, R.T., 1938, "Operational treatment of the nonuniform-lift theory in airplane dynamics", NACA Technical Note 667, 12pp. National Advisory Commitee for Aeronautics. Washington, DC.

Liang, C. and Rogers, C.A., 1997, "Design of shape memory alloy springs with applications in vibration control", Journal of Intelligent Material Systems and Structures. Vol.8, No.4, pp. 314-322.

Sousa, V.C., Anicézio, M.M., De Marqui Jr, C. and Erturk, A., 2011, "Enhanced aeroelastic energy harvesting by exploiting combined nonlinearities: theory and experiment", Smart Materials and Structures. Vol.20, No.9, pp. 094007 (8pp).

Sousa, V.C. and De Marqui Jr, C., 2016, "Effect of pseudoelastic hysteresis of shape memory alloy springs on the aeroelastic behavior of a typical airfoil section", Journal of Intelligent Material Systems and Structures. Vol.27, No.1, pp. 117-133.

Sousa, V.C., De Marqui Jr, C., Elahinia, M.H., 2016, "Effect of constitutive model parameters on the aeroelastic behavior of an airfoil with shape memory alloy springs", Journal of Vibration and Control. Published online before print July 25, 2016. 21pp.

RESPONSIBILITY NOTICE

The authors are the only responsible for the material included in this paper.